Shepherd, R. K., P. Carter, Y. L. Enke, A. K. Wise, and J. B. Fallon. 2018. Chronic intracochlear electrical stimulation at high charge densities results in platinum dissolution but not neural loss or functional changes in vivo. *Journal of Neural Engineering*. **16**(2): 026009.

doi: 10.1088/1741-2552/aaf66b

Chronic intracochlear electrical stimulation at high charge densities results in platinum dissolution but not neural loss or functional changes *in vivo*

Robert K. Shepherd[1,2], Paul M. Carter[3], Ya Lang Enke[3], Andrew K. Wise[1,2] and James B. Fallon[1,2]

[1]Bionics Institute, St Vincent's Hospital, Melbourne, Australia

[2]Medical Bionics Department, The University of Melbourne, Melbourne, Australia

[3]Cochlear Ltd., Sydney, Australia

Corresponding Author:

Prof Robert Shepherd,
Bionics Institute,
St Vincent's Hospital,
41 Victoria Parade,
Fitzroy, VIC 3065
Australia

Email: rshepherd@bionicsinstitute.org

Key words: Electrical stimulation, neural prosthesis, platinum electrode, stimulation safety, corrosion.

1. Abstract:

Objective: Although there are useful guidelines defining the boundary between damaging and non-damaging electrical stimulation they were derived from acute studies using large surface area electrodes in direct contact with cortical neurons. These parameters are a small subset of the parameters used by neural stimulators. More recently, histological examination of cochleae from patients that were long-term cochlear implant users have shown evidence of particulate platinum (Pt). The pathophysiological effect of Pt within the cochlea is unknown. We examined the response of the cochlea to stimulus levels beyond those regarded as safe, and to evaluate the pathophysiological response of the cochlea following chronic stimulation at charge densities designed to induce Pt corrosion. *Approach:* 19 guinea pigs were systemically deafened and implanted with a cochlear electrode array containing eight Pt electrodes of 0.05 0.075 or 0.2 mm^2 area. Animals were electrically stimulated continuously for 28 days using charge balanced current pulses at charge densities of 400, 267 or 100 $\mu C/cm^2$/phase. Electrically-evoked auditory brainstem responses (EABRs) were recorded to monitor neural function. On completion of stimulation electrodes were examined using scanning electron microscopy (SEM) and cochleae examined histology. Finally, analysis of Pt was measured using Energy Dispersive X-ray Spectroscopy (EDS) and inductively coupled plasma mass spectrometry *(*ICP-MS). *Main results:* Compared with unstimulated control electrodes and electrodes stimulated at 100 $\mu C/cm^2$/phase, stimulation at 267 or 400 $\mu C/cm^2$/phase resulted in significant Pt corrosion. Cochleae stimulated at these high charge densities contained particulate Pt. The extent of the foreign body response depended on the level of stimulation; cochleae stimulated at 267 or 400 $\mu C/cm^2$/phase exhibited an extensive tissue response that included a focal region of necrosis close to the electrode. Despite chronic stimulation at high charge densities there was no loss of auditory neurons (ANs) in stimulated cochleae compared with their contralateral controls. Indeed, we report a statistically significant *increase* in AN density proximal to electrodes stimulated at 267 or 400 $\mu C/cm^2$/phase. Finally, there was no evidence of a reduction in AN function associated with chronic stimulation at 100, 267 or 400 $\mu C/cm^2$/phase as evidenced by stable EABR thresholds over the stimulation program. *Significance:* Chronic electrical stimulation of Pt electrodes at 267 or 400 $\mu C/cm^2$/phase evoked a vigorous tissue response and produced Pt corrosion products that were located close to the electrode. Despite these changes at the electrode/tissue interface there was no evidence of neural loss or a reduction in neural function.

2. Introduction:

Although there are useful guidelines defining the boundary between damaging and non-damaging electrical stimulation, the so-called "Shannon limit" (1) was derived from acute stimulation studies using large surface area platinum (Pt) electrodes in direct contact with cortical neurons and stimulated at 50 pulses per second (pps). This boundary defines the maximum safe relationship between charge density and charge per phase for neural prostheses by the equation: $\log(Q/A) = k - \log(Q)$ where Q is the charge per phase (μC per phase), A is the geometric surface area of the stimulating electrode, Q/A is the charge density per phase (μC/cm^2/phase) and with the variable k within the range 1.5 – 1.85 (1-3). However, the parameters used to derive this relationship represent a small subset of the parameters used by neural stimulators operating in a clinical setting (4). While this equation provides a useful guideline for both manufacturers developing neural stimulators and regulatory agencies that approve these devices for clinical use, it does not accurately define safety levels for applications outside that subset. Important parameters including stimulus rate, electrode area, near- versus far-field electrodes, duty cycle, electrode material and the target neural population, will influence the boundary between safe and damaging electrical stimulation (3-5).

Cochlear implants are often considered the standard of care for individuals with profound to severe sensorineural hearing loss who do not derive benefit from amplification. They are representative of a neural prosthesis incorporating far-field electrodes, i.e. electrodes that do not make direct contact with their target neural population. The typical distance between an electrode array within the cochlea and their neural target, the primary auditory neuron (AN), is in the order of 0.2-1.0 mm (6). We sought to establish the response of the cochlea to chronic electrical stimulation over a range of charge densities, including levels considered to be beyond those regarded as safe as defined by Shannon (k=1.5; (1)) and the Association for the Advancement of Medical Instrumentation (AAMI) standard for commercial cochlear implants (defined as the Shannon limit (k=1.75) with a maximum charge density of 216 μC/cm^2/phase (7)), in order to re-evaluate the safe limits of stimulation for cochlear implants using Pt electrodes.

Platinum is regarded as a safe electrode material used in combination with carefully controlled charge-balanced current pulses operating within stimulus levels that allow charge injection via reversible Faradaic reactions (2, 3). However, high charge intensities or direct current can generate irreversible electrochemical reactions including water hydrolysis, Pt dissolution and O_2 reduction, altering the electrolyte environment adjacent to the electrode that may result in both tissue damage and electrode corrosion (8-13). Although the addition of bovine of human serum albumen has been shown to impede Pt dissolution (13, 14), this inhibition appears to be at the expense of the production of irreversible H_2 and O_2 evolution occurring at lower charge densities (13). In addition, more complex mixtures of proteins

found *in vivo* may act to increase the dissolution rate of Pt compared to inorganic electrolytes (15).

Significantly, recent studies involving the histological examination of cochleae taken from patients that were long-term cochlear implant users during their life-time, have shown evidence of particulate Pt within the tissue capsule surrounding the electrode array (16-18, 19). One study also reported evidence of fine Pt particles of nano dimensions within the proximity of the electrode array (17). The mechanism underlying the Pt dissolution together with the pathophysiological response, particularly in relation to AN survival, is unknown. Some reports have described an increased foreign body response associated with particulate Pt within the cochlea (18), although whether there is a causal relationship between Pt deposition and this response remains unclear. Therefore, a second objective of the present study was to evaluate the pathophysiological response of the cochlea in controlled *in vivo* experiments following chronic stimulation at high charge densities designed to induce Pt corrosion.

The observation of Pt corrosion products in cochleae of long-term implant users also has implications for other neural stimulators as the great majority of commercial devices use Pt electrodes and many use stimulus parameters that are significantly greater than the typical stimulus levels used in cochlear implants (4). Numerous preclinical studies have been performed by manufacturers of neuromodulation devices using different animal models and a broad range of stimulation parameters (including Shannon k > 1.85), while developing devices for clinical use (5).

Little is known about the toxicity or the systemic distribution of these corrosion products *in vivo*. There is, however, an extensive *in vitro* literature implicating Pt ions and complexes with cell toxicity. DNA appears the primary target of inorganic Pt compounds, underlying their known mutagenic properties (20). Moreover, Pt complexes such as Cisplatin have been used extensively as anticancer drugs and also exhibit toxic side effects including ototoxicity (21). Recently, an *in vitro* study demonstrated Pt cytotoxicity in two cell lines using either Pt ions generated by the corrosion of Pt electrodes following stimulation in saline, or Pt nanoparticles (22). Pt ions produced cell death at concentrations of 1.64 μg/ml, approximately two orders of magnitude lower than the levels of toxicity associated with Pt nanoparticles (100 μg/ml).

In the present study we describe the pathophysiological response of the deafened guinea pig cochlea following chronic electrical stimulation using smooth Pt electrodes. We used small laser cut electrode areas and a charge per phase of 0.2 μC to achieve charge densities of up to 400 $\mu C/cm^2$/phase (Shannon k ~ 1.9); levels beyond those regarded as safe limits for Pt electrodes (1, 7). While we observed Pt corrosion products in cochlear tissue following stimulation at these high charge densities, we report no adverse functional or degenerative changes to the target ANs.

3. Methods:

Experimental subjects

This study was performed using a total of 19 pigmented guinea pigs. All procedures were conducted with approval from the Bionics Institute Animal Research and Ethics Committee, and were performed in accordance with the Australian Code of Practice for the Care and Use of Animals for scientific purposes and followed the principles of the US National Institutes of Health guidelines regarding the care and use of animals for experimental procedures.

Auditory brainstem responses

All animals had otoscopically normal tympanic membranes and normal hearing determined by a click-evoked auditory brainstem response (ABR; threshold <50 decibels peak equivalent sound pressure level [dB p.e. SPL] re 20 μPa) (23). Under general anaesthesia (ketamine, 60mg/kg (Parnell Australia) and xylazine, 4mg/kg (Ilium, Australia); intramuscular injection), ABRs were recorded differentially using subcutaneous (s.c.) needle electrodes (vertex positive; neck negative; thorax ground). All recordings were made in a sound attenuated, electrically shielded room. Acoustic clicks of 100 μs duration were delivered by a calibrated speaker at intensities of up to 100 dB p.e. SPL. Click stimuli were presented at 25 per second, and the scalp recorded responses were amplified, filtered (5 Hz-1 kHz), recorded to computer and averaged over 100 trials at stimulus intensities from 100 dB p.e. SPL to below a threshold response. Threshold was defined as the smallest click amplitude required to evoke a peak-trough response of >0.5 μV for wave III of the ABR in two consecutive recordings.

Deafening protocol

All animals were ototoxically deafened. Under gaseous anaesthesia (1–2% isoflurane in oxygen, 1L/min; Isoflo; Zoetis, UK) the right jugular vein was exposed and cannulated by an intravenous injection of frusemide (130 mg/kg; Ilium, Australia), followed by kanamycin sulfate (420 mg/kg, s.c.; Sigma-Aldrich, USA) within 2 minutes of frusemide administration (24). This deafening technique produces a highly symmetrical bilateral sensorineural hearing loss (23, 24). Animal weight and behaviour were closely monitored following deafening. Seven days following this deafening procedure the hearing status of each animal was re-tested. Only animals that exhibited a 50 dB increase in their click-evoked ABR threshold were included in this study.

Scala tympani electrode array

Modified HL8 research electrode arrays (HL8), manufactured by Cochlear Ltd. and specifically designed for use in guinea pigs, were used in the present study. This array consists of 8 half-band Pt electrodes (Fig. 1) with electrode 1 (E1) the most basal and electrode 8 (E8) the most apical (Fig. 1a). This electrode array is designed to be atraumatically inserted into the upper basal turn of the guinea pig scala tympani. Each Pt

electrode was connected via a leadwire to a battery powered stimulator (details below) located in a backpack.

Because both charge density and charge per phase are co-factors associated with neural damage (1, 25) we elected to hold charge per phase constant (0.2 μC/phase) while varying charge density by varying the geometrical surface area of the Pt contacts. Each electrode array had exposed Pt contact areas of 0.05, 0.075 or 0.2 mm^2 manufactured via laser ablation of a region of polydimethylsiloxane (PDMS) overlaying each Pt electrode (Fig. 1b-d). A previous cytotoxicity study has demonstrated that laser ablation of PDMS has a negligible effect on the biological response of adjacent cells (26). Finally, although smaller electrodes have a larger perimeter to surface area ratio that can contribute to more pronounced edge effects, the electrodes used in the present study were recessed, substantially mitigating this effect by producing a more uniform current density over the electrode surface (27).

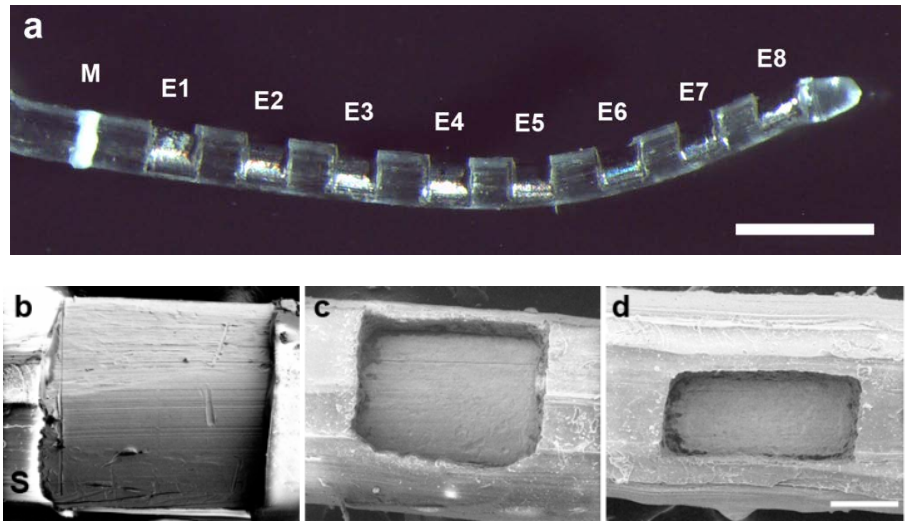

Figure 1. *(a) Low power micrograph of a HL8 research electrode array illustrating the 8 Pt electrodes (E1-E8) on the array. All Pt contact areas on each array were identical. The white band (M) is used as a surgical guide to ensure a uniform insertion depth for each electrode array. Scale bar = 1 mm. (b) – (d) Scanning electron micrographs illustrating the three Pt contact areas used in this study. (b) 0.2 mm^2; (c) 0.075 mm^2; (d) 0.05 mm^2. S = PDMS silicone. Scale bar = 100 μm.*

Cochlear implant surgery

Two weeks following deafening each animal was anesthetized with isoflurane 2–2.5% in oxygen (1L/min). Surgery was performed under sterile conditions with the animal's temperature maintained at 37°C using a heating pad. A left dorsal bulla approach was used and the malleus and incus were removed to expose the left cochlea. The round window membrane was incised and the electrode array was inserted into the scala tympani. The round window was sealed with muscle, the leadwire proximal to the electrode array was fixed inside the bulla using dental cement (Duralon; Germany), and the distal leadwire exited the skin via a small incision in the back of the neck. The wounds were sutured in two

layers with Coated Vicryl 3-0 (Ethicon Inc., USA). Each animal was given Hartmann's solution (10ml/kg; s.c.). The antibiotic Baytril (0.10mg/kg, s.c.; Bayer, Germany), and the analgesic Temgesic (50 mg/kg, s.c.; Reckitt-Benckiser, UK) were given after surgery and on the next day to aid recovery. No surgery was performed on the right cochlea; they served as deafened, untreated controls.

Electrode impedance

In order to monitor the status of the intracochlear electrodes, the impedance of each electrode was measured in a bipolar configuration throughout the chronic stimulation period (28). The impedance was monitored by delivering a 100 μA biphasic current pulse of 100 μs pulse-width and recording the peak of the voltage transient during the first phase.

Electrically-evoked auditory brainstem responses

Electrically-evoked auditory brainstem responses (EABRs) were recorded to monitor neural function. These responses provide an effective physiological indicator on the status of the ANs (23). EABRs were recorded immediately following implant surgery and on completion of the 28 day electrical stimulation program using the same recording configuration as ABRs (23). Biphasic current pulses (100 μs per phase; 50 μs interphase gap) were used to stimulate selected bipolar electrodes along the intracochlear electrode array (E1-E2, E2-E3, E3-E4, E4-E5, E5-E6, E6-E7, E7-E8). One hundred presentations were averaged for each recording. Two sets of recordings were made at each current level. Recordings were made at intensity intervals presented randomly from below threshold to a maximum of 250 Current Level (CL; where current in mA = 17.5 x ($100^{(CL/255)}$)).

Chronic stimulation program

Immediately following the post-operative EABR recordings each animal commenced a chronic stimulation program using a custom built back-pack stimulator (29) that delivered 100 μs/phase charge balanced biphasic current pulses at 200 pps and developing a charge/phase of 0.2 μC/phase via a tripolar electrode configuration. In this configuration a cathodic first phase current is delivered on the centre electrode of the tripole while the two flanking electrodes are connected together to provide the return path. All currents are then reversed in phase two of the pulse. Tripolar configuration was used since it recruits relatively small numbers of auditory neurons compared to monopolar stimulation (30), allowing higher charge levels to be passed within the animals' comfortable range. In the present study, centre electrodes generated charge densities of 100, 267 or 400 $\mu C/cm^2$/phase (E4 and E7; Table 1) while the flanking electrodes developed half the charge density of each tripole centre electrode (E3, E5, E6 and E8; Table 1). Charge-balance was achieved using electrode shorting between current pulses (31). Each animal was continuously stimulated for 28 days. An additional cohort of 4 animals was unilaterally implanted with a HL8 research electrode array for 28 days but did not receive any electrical stimulation.

Table 1: Summary of the cohorts used in this study

Cohort	Pt contact area* (mm^2)	Charge per phase (μC/phase)	Centre electrode** charge density ($\mu C/cm^2$/phase)	Flanker electrode charge density ($\mu C/cm^2$/phase)	N (cochleae)
1	0.05-0.2	0	0	0	4
2	0.2	0.2	100	50	5
3	0.075	0.2	267	133	5
4	0.05	0.2	400	200	5

Notes: *Geometrical surface area. **Here and throughout this publication, unless otherwise stated, the charge density refers to that on the centre electrode of the tripole.

Histology

At the end of the 28 day stimulation program all animals were euthanized with sodium pentobarbitone and systemically perfused with heparinised normal saline at 37^{o}C followed by 10% neutral buffered formalin (NBF) at 4^{o}C. The electrode array was removed for examination under a scanning electron microscope (SEM; see below) and both the stimulated and contralateral control cochleae postfixed for 1 h and washed three times in NBF at room temperature (32). Cochleae were decalcified in 10% (wt/vol) ethylene diamine tetra-acetic acid for two weeks, cryoprotected with 15%, then 30% sucrose overnight, before being infiltrated and embedded in Tissue-Tek O.C.T. cryosectioning compound (Sakura, Japan), snap frozen and stored at -80°C. Cochleae were sectioned at 12µm to the mid-modiolar point (Fig. 2) using a CM 1900 UV cryostat (Leica, Germany) at -22°C and sections were mounted onto Superfrost-Plus slides (Menzel-Gläser, Braunschweig, Germany). The remaining half of the cochlea was kept for trace analysis of Pt using inductively coupled plasma mass spectrometry (ICP-MS; see below).

A representative series of cochlear sections were stained with Mayer's haemotoxylin and Putt's eosin (H&E) for qualitative examination (32). In addition a number of sections were selected for CD 163 immunostaining for macrophages (19). Briefly, sections were rinsed in phosphate buffered saline (PBS) and incubated in 5% normal goat serum followed by the primary antibody (anti-human CD 163 diluted 1:500) overnight at 4^{o}C. Sections were then rinsed in five washes of PBS before applying the secondary antibody (Biotinylated anti-mouse diluted 1:250) for 4 hours at room temperature. After rinsing in PBS the sections were incubated in Avidin-Biotin horseradish peroxidase (ABC kit; Vector Labs, Burlinggame, USA) for 30 minutes at room temperature and rinsed in PBS. Colourization was accomplished in 0.01% diaminobenzidine for 2-5 minutes then rinsed in 0.01% H_2O_2. The sections were then dehydrated in graded alcohols and cover slipped.

The extent of auditory nerve survival, measured as AN density, and the foreign body tissue response within the scala tympani were quantified and compared statistically with data from the contralateral unimplanted control cochlea and the implanted unstimulated control

cochleae. ANs were quantified in mid-modiolar sections using a Zeiss Axioplan microscope by a single observer blinded to the experimental cohorts. ANs were identified within Rosenthal's canal and counted within the lower basal (LB), upper basal (UB), lower middle (LM), upper middle (UM) and the apical (A) cochlear regions (32). Only ANs exhibiting a clear nucleus were counted. The area of Rosenthal's canal was measured using Image J software and the density of the ANs was determined. The AN density for each cochlear region was averaged from 5 sections that were spaced at least 72 µm apart, ensuring that no AN was counted more than once.

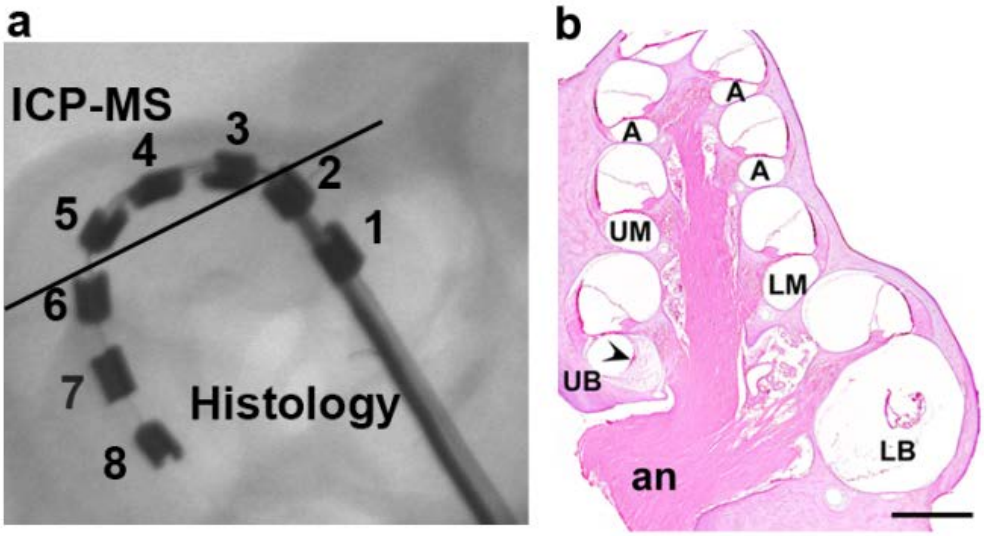

Figure 2. *(a) An x-ray image of a HL8 research electrode array implanted into the basal turn of the guinea pig scala tympani. The location of the 8 Pt electrodes are indicated. Half the cochlea was sectioned for histological evaluation in the plane of the solid line. This orientation provided histological analysis of the tissue response adjacent to electrodes E1 and E2 (unstimulated controls), and electrodes E6, E7 and E8 (chronic tripolar stimulation centred on E7). The remaining portion of the cochlea, representing tissue adjacent to electrodes E3, E4 and E5 (chronic tripolar stimulation centred on E4), was used for trace analysis of Pt using inductively coupled plasma mass spectrometry (ICP-MS). (b) Mid-modiolar micrograph of a cochlea that has been chronically implanted with an electrode array in the lower (LB) and upper (UB) basal turn scala tympani, and stimulated at a charge density of 400 µC/cm^2/phase. The figure illustrates the five cochlear regions used for analysis of tissue response and AN survival; lower basal turn (LB), adjacent to control electrodes E1 and E2; upper basal turn (UB), adjacent to the stimulating electrodes E6, E7 and E8; lower middle turn (UM), apical to the electrode array; upper middle turn (UM) and the apical region of the cochlea (A). A fine tissue capsule is evident in the LB turn, an extensive tissue response associated with the electrical stimulation is present in the UB turn (arrowhead), while there is a minimal tissue response in the LM turn or above. an = auditory nerve. Scale bar = 1 mm.*

In order to quantify the foreign body response the extent of fibrosis in the cochlea was measured in H&E stained sections at six locations along the electrode array (two each in the LB, UB and LM turns; Fig. 2b). An image of the scala tympani was captured and its area measured. The 'Triangle' algorithm in Image J was used to threshold the image in order to quantify the tissue response. The area of scala tympani excluding the area of the electrode array, was measured and the proportion of the scala tympani occupied by the tissue response calculated. The extent of the tissue response associated with implantation and chronic stimulation at the three charge densities was compared statistically with the implanted, unstimulated control cochlea (cohort 1; Table 1).

The tissue capsule surrounding each electrode array was carefully examined and the nature of the inflammatory reaction associated with the tissue response assessed. In some cochleae particulate material of a metallic nature was observed within the tissue capsule. Both H&E and CD 163 immunostained sections were used to examine the response of macrophages to this particulate material. Finally, unstained histological sections from cochleae exhibiting particulate material were examined under the SEM and Energy Dispersive X-ray Spectroscopy (EDS) was used to identify the material (see below).

Scanning Electron Microscopy

Following removal from the cochlea, each electrode array was rinsed and ultrasonically cleaned in distilled water then stored in 70% ethanol before being examined for evidence of Pt corrosion using a FEI QUANTA 200 SEM. All 8 Pt electrodes on each electrode array were photographed at low (x 600) and medium (x 2000) magnification. A region of each electrode surface was then randomly selected and photographed at higher magnifications (x 4000 and x 10,000). The surface condition of each Pt electrode was evaluated by an investigator blinded to the experimental groups. Surface features, including mechanical damage, pitting corrosion, intergranular corrosion and surface deposits, were evaluated and the severity of Pt corrosion was graded from 0 (no corrosion); 1 (no evidence of corrosion but electrode at least partially coated with organic material); 2 (localized minor corrosion); 3 (localized moderate corrosion); 4 (widespread corrosion); 5 (severe and extensive corrosion) (33).

Representative unstained cochlear sections were examined under the SEM in an attempt to identify particulate matter observed within the fibrous tissue capsule of some cochleae. Specific sites associated with the tissue capsule were selected for elemental analysis using an INCA X-Act SDD EDS system with an Oxford Aztec Microanalysis System (3.1). Regions of the fibrous tissue capsule containing the particulate material were compared with regions only containing fibrous tissue.

Trace analysis of platinum

The un-sectioned half of each cochlea in cohort 4 (400 $\mu C/cm^2$/phase; Fig. 2a) was measured for Pt using ICP-MS by the National Measurement Institute of the Australian Government. Both the contralateral (unimplanted) control cochleae from this cohort and

cochleae from cohort 1 (implanted, unstimulated controls) were also examined for Pt using this technique. Each tissue sample was washed and stored in de-ionised water. Because tissue samples were required to be > 0.5 g we combined cochlea tissue from each cohort into a single analysis sample. Each sample was homogenized and digested in re-distilled nitric acid and hydrochloric acid (3:1) for 60 min in a DigiPrep block set (SCP Science) at 95^{o}C and transferred to a Milestone microwave for 30 min to complete the digestion process. Liquid samples were micro filtered and analysed using an Agilent 7700X ICP-MS system. Pt trace analysis was reported as the mean mass of Pt per half cochlea.

Statistical analysis

Evoked potential and electrode impedance data were examined statistically by comparing the stimulated versus the unstimulated control cochleae using a 2 way analysis of variance (ANOVA; electrode and time). Statistical comparisons of AN density were made by comparing each region of the stimulated cochlea with its unstimulated control cochlea using a paired-test. Finally, statistical comparison of the extent of fibrous tissue within the scala tympani and the degree of Pt electrode corrosion were performed using Kruskal-Wallis 1 way ANOVA (stimulated versus controls), with post hoc comparisons made using Dunn's method. Data are presented as mean and standard error of the mean (sem).

Results:

3.1. Electrode impedance

Figure 3 illustrates the mean electrode impedance of all chronically stimulated electrodes in the present study. Impedances were recorded immediately post-surgery (T0) and on completion of the stimulation program (T4). While there was a general increase in impedance as the electrode contact area reduced from 0.2 (Fig. 3a) – 0.05 mm^2 (Fig. 3c), there was no statistically significant difference between the pre- and post-stimulus impedances for each of the three chronically stimulated cohorts (100 μC/cm^2/phase: $p = 0.665$, n=30; 267 μC/cm^2/phase: $p = 0.476$, n=31; 400 μC/cm^2/phase: $p = 0.679$, n=15; paired t-Test).

3.2. Electrically-evoked responses

EABR thresholds for each animal were determined at implantation and on completion of the stimulation program to monitor for evidence of stimulus induced changes in AN function. Representative EABRs from one animal recorded prior to and following chronic stimulation at 400 μC/cm^2/phase are illustrated in Fig. 4a&b. These responses maintained typical waveform morphology and exhibited little change in threshold over the duration of the stimulation program. The mean EABR thresholds at both time points for all animals in the study are illustrated in Fig. 4 c&d. In all three chronically stimulated cohorts, lower EABR thresholds were evident for more apical electrodes, reflecting the closer proximity of these electrodes to ANs due to the tapered nature of the scala tympani. Importantly, there was no statistically significant difference in EABR threshold between pre- and post-stimulation EABR

thresholds for any chronically stimulated cohort (100 μC/cm^2/phase: p = 0.974, n=26; 267 μC/cm^2/phase: p = 0.492, n=31; 400 μC/cm^2/phase: p = 0.277, n=29; paired t-Test).

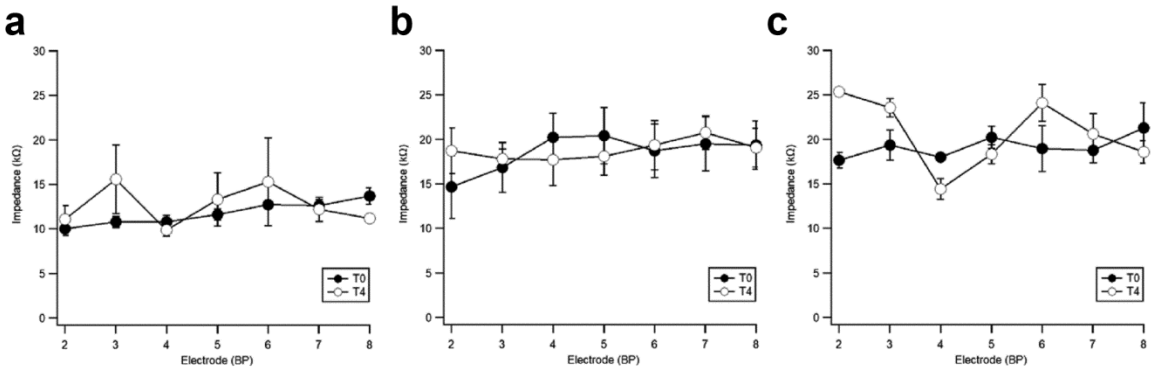

Figure 3. *Electrode impedance measured immediately post-surgery (T0) and on completion of the chronic stimulation program (T4) for (a) 100 μC/cm^2/phase, (b) 267 μC/cm^2/phase and (c) 400 μC/cm^2/phase cohorts. There was no statistically significant difference in impedance between pre- and post-stimulation impedances for any stimulated cohort (paired t-Test). Error bars = ± sem.*

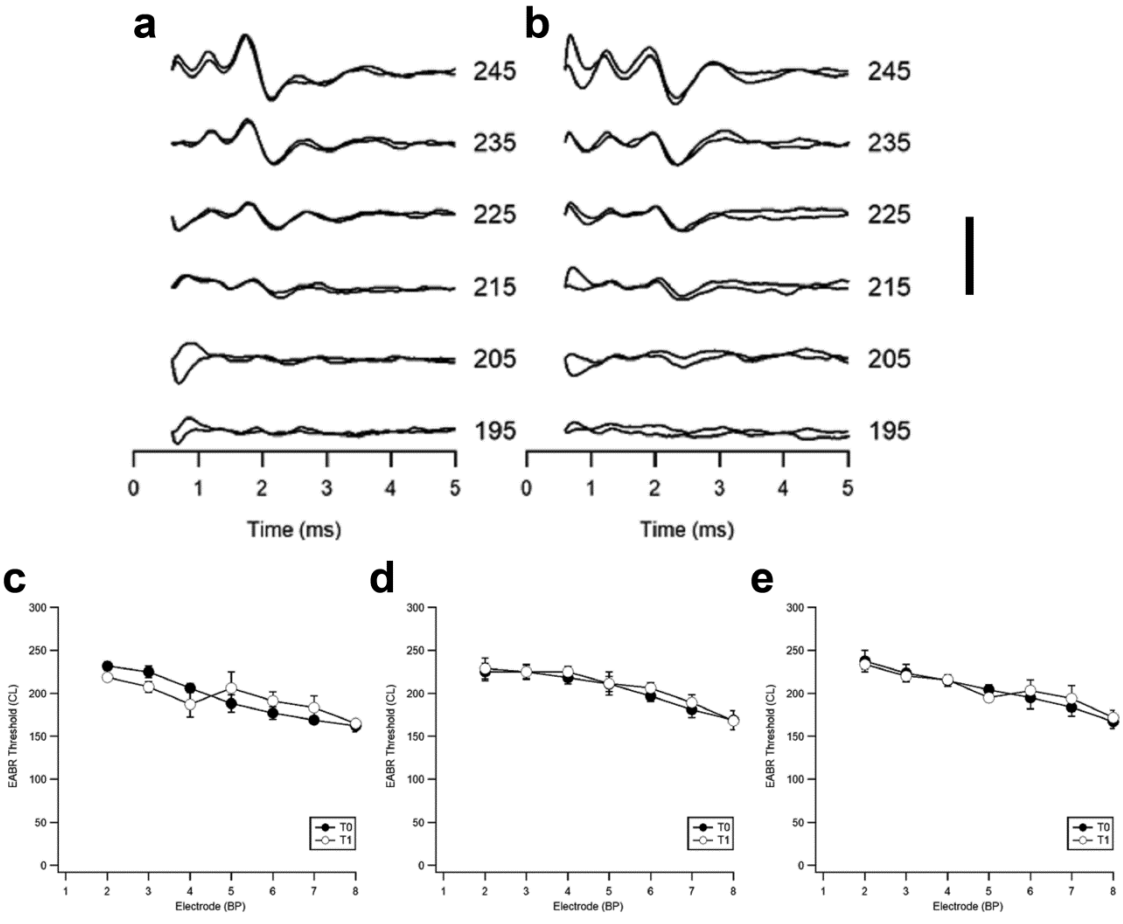

Figure 4. *Representative EABRs recorded (a) immediately post-surgery and (b) on completion of the chronic stimulation program from an animal chronically stimulated at 400 μC/cm^2/phase. EABRs were evoked by a charge balanced biphasic current pulse of 100 μs/phase. Current amplitude is in current level (CL). Two responses are plotted at each stimulus level and the first 0.5 ms of each trace, containing the stimulus artefact, has been removed. Scale bar = 5 μV. (c)-(e) Mean electrically-evoked auditory brainstem response thresholds measured immediately following surgery (T0) and on completion of the chronic stimulation program (T4) for all animals stimulated at (c) 100 μC/cm^2/phase, (d) 267 μC/cm^2/phase and (e) 400 μC/cm^2/phase. There was no statistically significant difference in EABR threshold between pre- and post-stimulation impedances for any cohort (Paired t-Test). Error bars = ± sem.*

3.3. Cochlear pathology

3.3.1. General cochlear pathology

There was no evidence of electrode insertion trauma, including fractures of the osseous spiral lamina or perforations of the basilar membrane, in any histological section examined. Any tissue reaction was therefore in response to the chronically implanted electrode array and/or the effects of the electrical stimulation.

3.3.2 Tissue response

Figure 5 illustrates the typical tissue response observed in the UB turn adjacent to an electrode array for the four chronically implanted cohorts in the present study. Implanted, unstimulated control cochleae exhibited a minimal tissue response within the scala tympani with typically no evidence of a tissue capsule surrounding the electrode array (Fig. 5a). A relatively fine, mature fibrous tissue response was always evident in the UB turn of chronically stimulated cochleae. This typically took the form of a thin, mature tissue capsule surrounding the electrode array forming an electrode tract (ET; Fig. 5b-d), with loose vascularized fibrous tissue occupying much of the remainder of the scala tympani. In general, a more extensive tissue response was associated with higher stimulus intensity (compare Fig. 5b with Fig. 5c or d). Finally, there was no evidence of new bone formation in any cochlea in this study.

We quantified the tissue response in each chronically implanted cochlea by measuring the area of tissue occupying the scala tympani in the LB, UB and LM turns (Fig. 6). The data demonstrate the significant increase in tissue response associated with electrical stimulation in the UB turn (UB; Fig. 6). The degree of tissue response in the UB turn was related to the stimulus level and was restricted to the site of stimulation; there was little evidence of a tissue response just apical to the electrode array (LM; Fig. 6). Moreover, there were relatively small amounts of tissue growth adjacent to the unstimulated section of the electrode array in the LB turn (LB; Fig. 6).

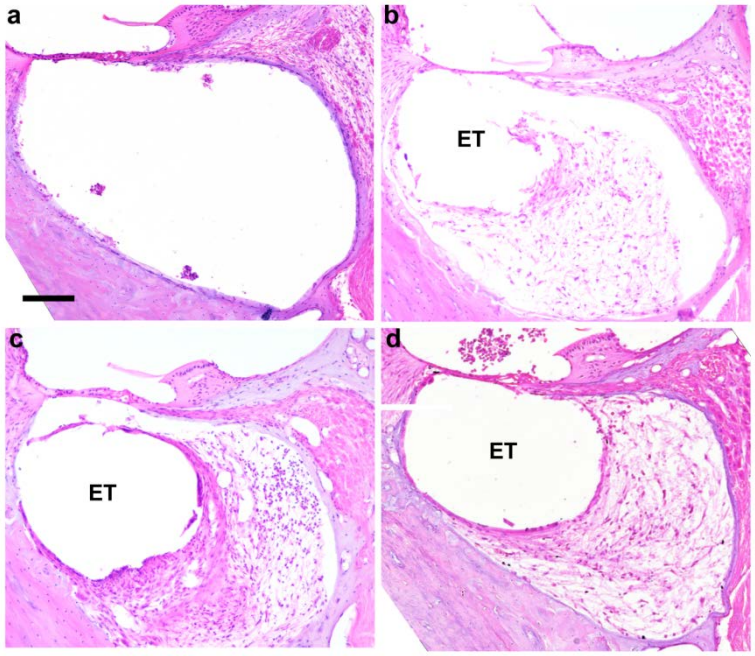

Figure 5. *Representative micrographs illustrating typical tissue response within the UB turn of the scala tympani. (a) Implanted unstimulated cochleae exhibited a minimal tissue response. All stimulated cochleae exhibited a tissue response with the most extensive response evident in cochleae stimulated at higher charge densities. (b) 100, (c) 267, (d) 400 μC/cm^2/phase. ET = electrode tract. Scale bar = 100 μm.*

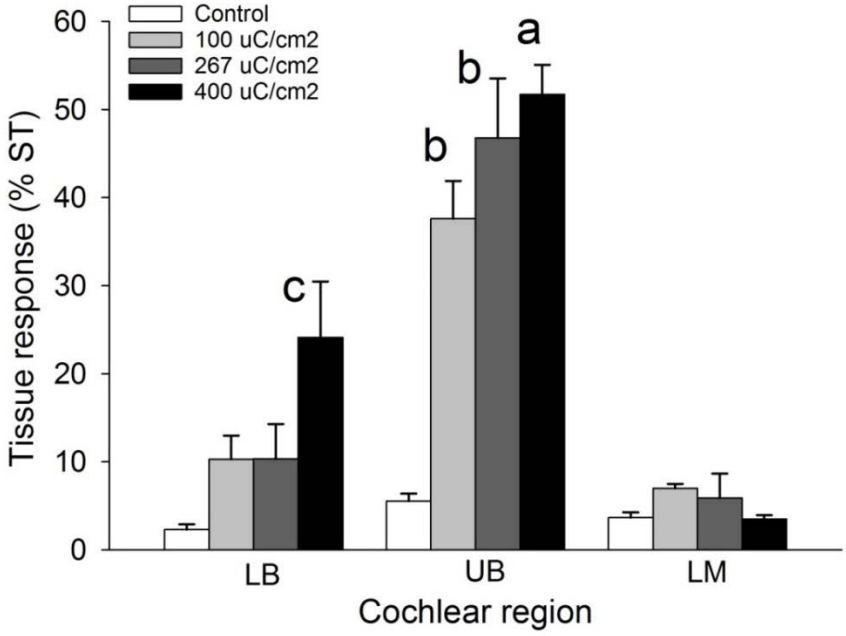

Figure 6. *The extent of tissue response occupying the scala tympani (ST) in cochlear regions LB, UB & LM for the four chronically implanted cohorts in this study. There was a statistically significant difference in fibrous tissue response for both charge density (p<0.001) and cochlear region (p<0.001) with a significant interaction between charge density and region (p<0.001; two-way ANOVA, charge density x cochlear region). Holm-Sidak post hoc analysis: a = significant difference with all cohorts in LB and LM, and control (p<0.001) and 100 μC/cm^2/phase in UB (p<0.01); b = significant difference with control 100 and 267 μC/cm^2/phase in LB, and control, 100, 267 and 400 μC/cm^2/phase in LM (p < 0.001); c = significant difference with 400 μC/cm^2/phase in LM (p < 0.05).*

In addition to this mature fibrous tissue response, histological examination of cochleae stimulated at 267 or 400 μC/cm2/phase exhibited focal regions of necrosis associated with the tissue capsule (Fig. 7). Included in these regions of necrosis were zones of amorphous acellular material which were typically surrounded by a band of macrophages and plasma cells. This pathology had developed and persisted over weeks, as evidenced by the mature tissue debris, fibrosis and the absence of neutrophils. No bacteria were observed. The remaining scala tympani typically contained numerous fibroblasts, additional inflammatory cells and mature fibrous tissue. Finally, the location and dimensions of these focal necrotic zones were consistent with the size of the Pt electrode contact.

Figure 7. *A micrograph illustrating a focal region of necrosis (arrowheads) within an otherwise mature electrode tissue capsule. The necrotic region was associated with amorphous material and surrounded by a band of cells including macrophages and plasma cells (arrows). The lumen of the scala tympani was typically occupied by mature fibrous tissue (f). The dimensions of these necrotic foci suggest that this region of tissue was in contact with a stimulating electrode. This necrotic response was only observed in cochleae stimulated at 267 or 400 μC/cm^2/phase. ET = electrode tract; * = blood vessel. Scale bar = 100 μm.*

3.3.3 AN survival

Figure 8 illustrates the typical AN survival in the UB turn (i.e. adjacent to the stimulating electrodes) in cohorts 1-4 in this study. The relatively low packing density of ANs in the right control cochleae (Fig. 8b, d, f & h), illustrate the typical degeneration of ANs observed following a sensorineural hearing loss (34). Compared to the close symmetry associated with AN survival in the implanted unstimulated control (compare Fig. 8a & b), the stimulated cochleae (Fig. 8c, e & g) appear to exhibit greater AN survival than their contralateral control cochleae.

Quantitative analysis of AN survival showed a statistically significant *increase* in AN survival adjacent to chronically stimulated electrodes in the UB turn versus their contralateral control cochlea at charge densities of 267 and 400 μC/cm^2/phase (Fig. 9). Cochleae stimulated at 100 μC/cm^2/phase exhibited a small but non-significant increase in AN survival proximal to the site of stimulation. In the unstimulated control cochlea there was a statistically significant increase in AN survival in the apical turn compared with the contralateral control cochlea. The remaining cochlear turns of all cohorts showed close bilateral symmetry of AN survival, consistent with the highly symmetrical pattern of AN degeneration associated with systemic deafening (23, 24).

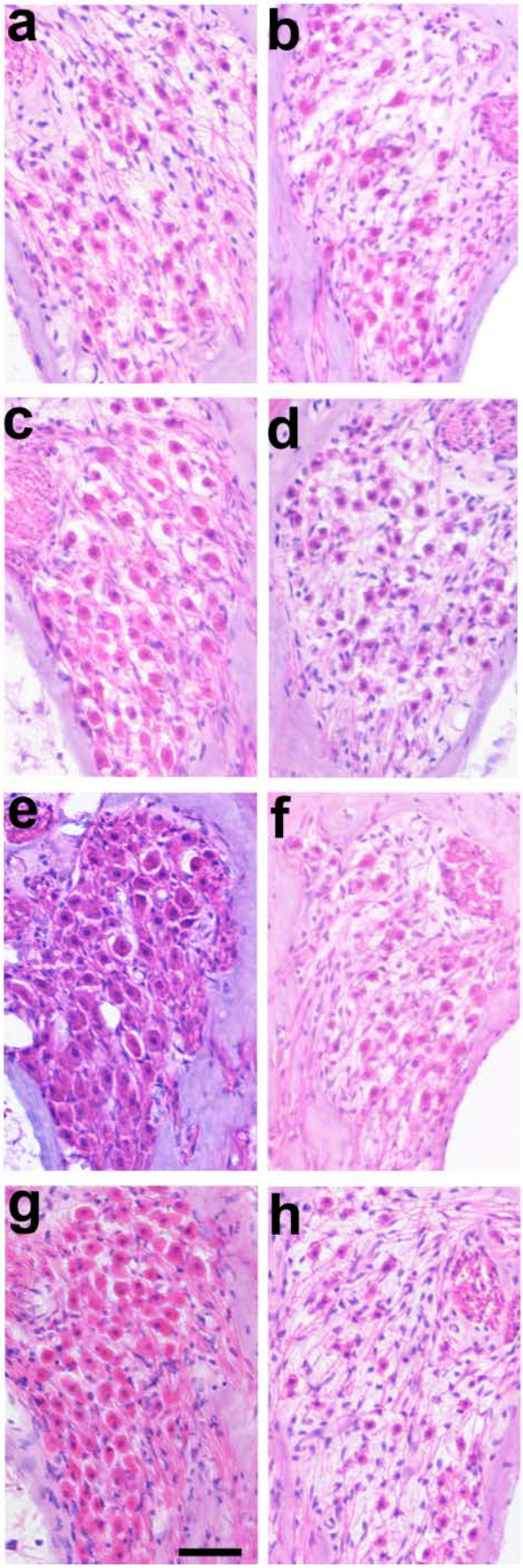

Figure 8. *Representative micrographs of Rosenthal's canal from the UB turn illustrating the extent of AN survival in each of the 4 chronically implanted cohorts (a, c, e, g) compared with their contralateral controls (b, d, f, h). (a) Implanted unstimulated control; (b) 100 $\mu C/cm^2$/phase; (c) 267 $\mu C/cm^2$/phase; (d) 400 $\mu C/cm^2$/phase. There was an increase in AN survival in the UB turn of the chronically stimulated cochleae compared to their contralateral control cochlea (compare 8c, e & g with 8d, f & h). Scale bar = 50 μm.*

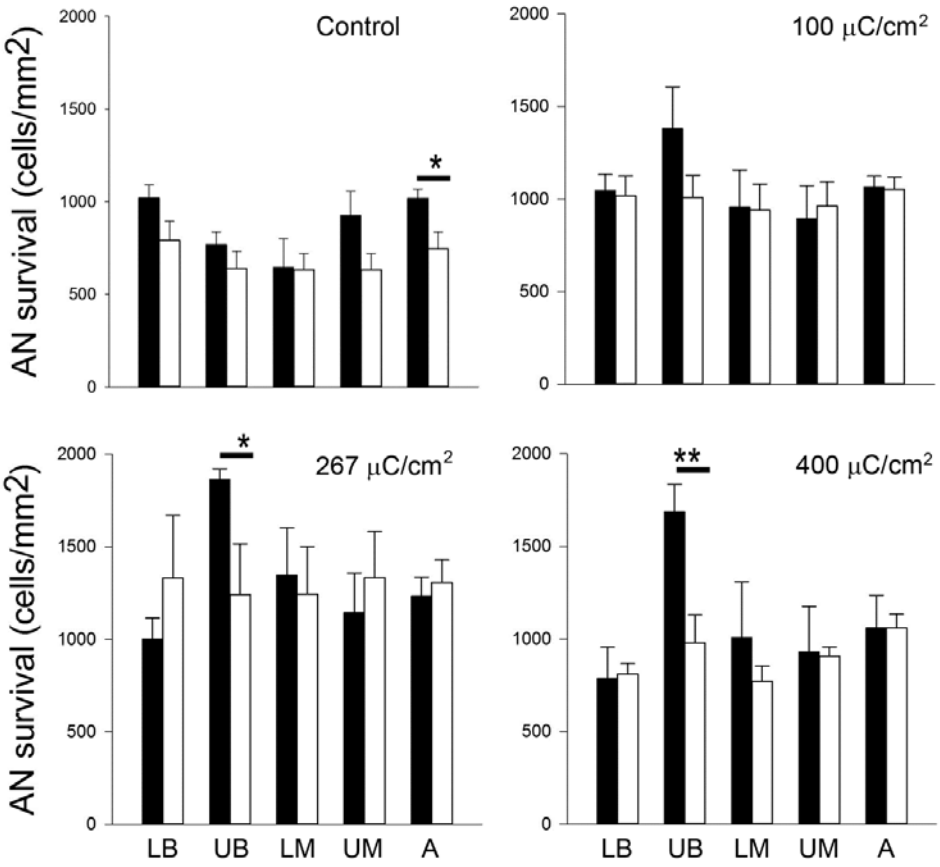

Figure 9. *Mean AN density for both the implanted and contralateral control cochleae for each cohort in this study (black bars = implanted; open bars = contralateral controls). AN density was greater in the UB turn (i.e. the site of stimulation) of the three stimulated cohorts compared with their paired control. This difference was statistically significant at 267 and 400 μC/cm^2/phase. There was also a statistically significant difference in the apical region of the unstimulated control cochleae, however there was no statistically significant difference in any other region of control or stimulated cochleae (i.e. LB, LM, UM and A turns). * p < 0.05; ** p < 0.01 (Paired t-test; Error bar = sem).*

3.4 Electrode corrosion

Scanning electron microscopy of the electrode provides high magnification topographical examination of the Pt surface for evidence of corrosion (2). Representative micrographs from four electrodes on an array stimulated continuously for 4 weeks at 400 μC/cm^2/phase (cohort 4), illustrate the range in Pt corrosion observed in the present study (Fig. 10). Electrode E1 served as an unstimulated control electrode; despite manufacturing marks on its surface, this electrode showed no evidence of corrosion (corrosion grade 0; Fig. 10a). Electrode E5 served as a flanker electrode and was therefore stimulated at 200 μC/cm^2/phase. This electrode exhibited minimal evidence of Pt corrosion (grade 1; Fig. 10b). Electrodes E4 and E7 served as centre electrodes for the two tripolar stimulation sites and were stimulated at 400 μC/cm^2/phase. Both electrode surfaces exhibited widespread pitting corrosion (grade 4; Figs. 10c & d).

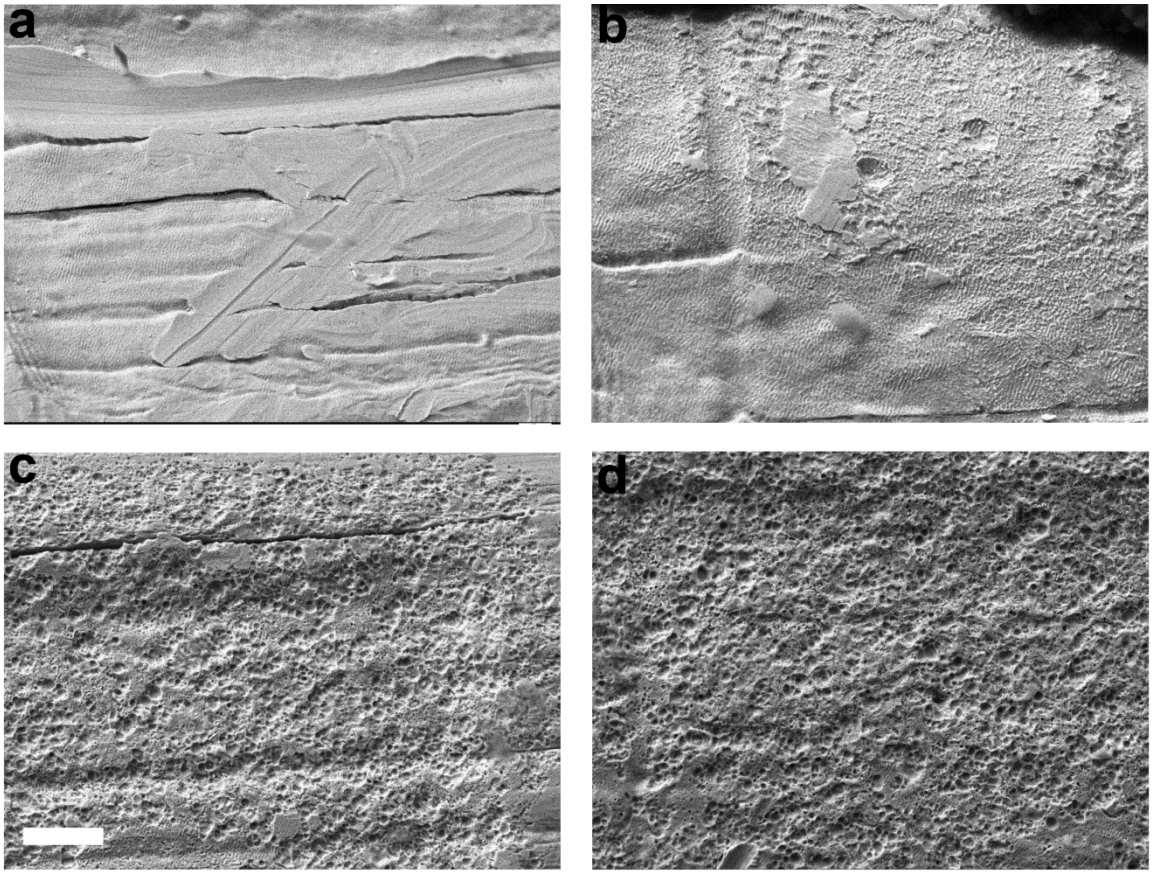

Figure 10. *SEM images illustrating the electrode surface of four Pt electrodes taken from an electrode array chronically stimulated at 400 μC/cm^2/phase. Centre electrodes of the tripole therefore received cathodic first phase stimulation at 400 μC/cm^2/phase and flanker electrodes received anodic first phase stimulation at 200 μC/cm^2/phase. (a) Electrode E1 was unstimulated for the duration of the 4 week implantation period. While the electrode exhibited surface features associated with manufacturing, there was no evidence of corrosion. (b) Electrode E5 was a flanker electrode on a tripolar array. There was minimal evidence of Pt corrosion on the electrode surface. Electrodes E4 (c) and E7 (d), both centre electrodes on tripolar arrays and stimulated at 400 μC/cm^2/phase for the duration of the study, showed extensive pitting corrosion across their electrode surfaces. Scale bar = 20 μm.*

Figure 11 shows the surface features of four E4 Pt electrodes illustrating the effects of charge density on Pt corrosion. There is no evidence of corrosion associated with either an unstimulated control electrode (grade 0; Fig. 11a) or an electrode chronically stimulated at 100 μC/cm^2/phase (grade 0; Fig. 11b). In contrast stimulation at 267 (grade 4; Fig. 11c) or 400 μC/cm^2/phase (grade 4; Fig. 11d) resulted in widespread Pt corrosion.

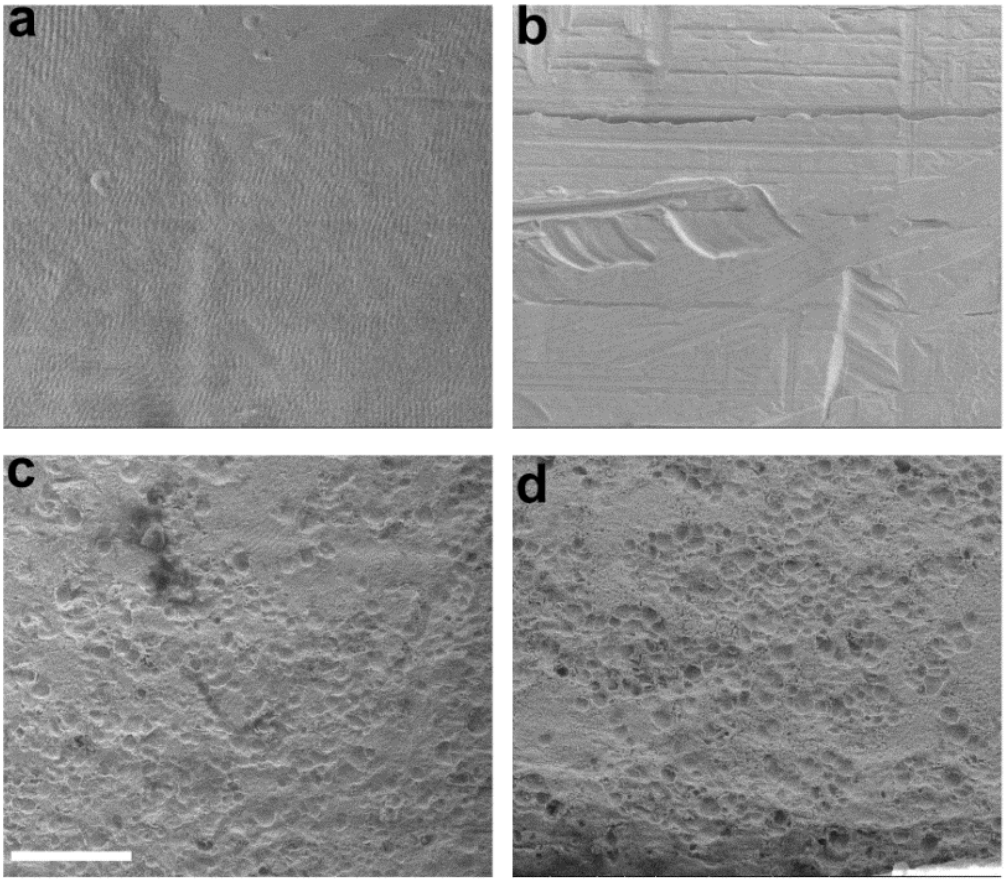

Figure 11. *Representative SEM micrographs of centre tripolar electrode E4 from each chronically implanted cohort. (a) implanted control electrode; (b) stimulated at 100 $\mu C/cm^2$/phase; (c) stimulated at 267 $\mu C/cm^2$/phase; and (d) stimulated at 400 $\mu C/cm^2$/phase. There was no evidence of Pt corrosion on the control electrode or the electrode stimulated at 100 $\mu C/cm^2$/phase. In contrast, there was significant pitting corrosion on the electrodes stimulated at 267 and 400 $\mu C/cm^2$/phase. Scale bar = 20 μm.*

We compared the SEM surface grading of the electrodes within each cohort (Fig. 12). There was no significant difference across electrodes for both the control ($p=0.84$; $n=4$) and 100 $\mu C/cm^2$/phase cohorts ($p=0.60$; $n=5$ ANOVA by Ranks). Corrosion grades for these two cohorts varied between 0 (no corrosion) and 1 (no corrosion however evidence of some organic coating over part of the electrode surface). In contrast, there were statistically significant differences in corrosion grading across electrodes in both the 267 ($p<0.001$; $n=5$) and 400 $\mu C/cm^2$/phase ($p<0.001$; $n=5$) cohorts. Electrodes E4 and E7 (centre tripolar electrodes) in both cohorts exhibited corrosion grades of between 3 (localized moderate corrosion) and 5 (extensive corrosion) which were significantly greater than all other electrodes in each cohort ($p<0.05$; Dunn's post hoc analysis). In addition, the flanker electrodes E3, E5, E6 and E8 in the 400 $\mu C/cm^2$/phase cohort (grades 1-3) exhibited significantly greater levels of corrosion compared with control electrodes E1 and E2 ($p<0.05$; Dunn's post hoc analysis).

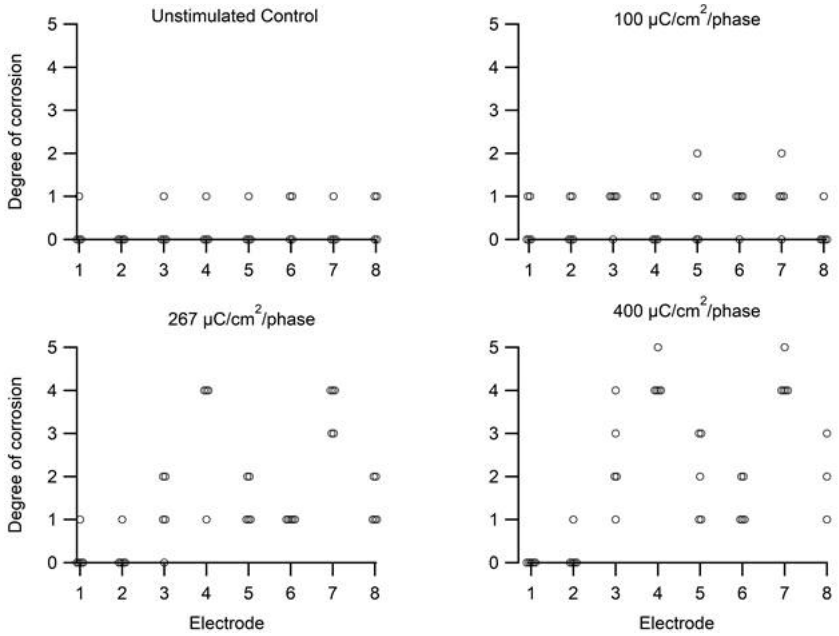

Figure 12. *Corrosion grade for each electrode in this study. There was minimal evidence of corrosion in the unstimulated controls and electrodes stimulated at 100 µC/cm^2/phase (grades 0-1). More extensive Pt corrosion was observed associated with electrodes stimulated at 267 and 400 µC/cm^2/phase. The degree of corrosion in these two cohorts was most extensive on the centre electrodes of each tripole (grades 4-5; E4 & E7), while reduced levels of corrosion were evident on their flanker electrodes (grades 2-3; E3, E5, E6 & E8). The unstimulated control electrodes in these cohorts exhibited minimal corrosion (grades 0-1; E1 & E2). While five electrode arrays were analysed in each cohort, occasionally an individual electrode on an array was not recovered (e.g. electrode 8, 400 µC/cm^2/phase). See text for statistical significance.*

3.5 Analysis of particulate deposits

In cochleae stimulated at 267 or 400 µC/cm^2/phase, particulate matter was apparent in the electrode-tissue capsule of the UB turn proximal to the chronically stimulated tripolar electrodes centred on electrode E7. This material was typically localized close to the electrode tract, particularly in the vicinity of the focal necrotic response (Fig. 13). There was no evidence of particulate deposits in the tissue capsule associated with control electrodes (E1 & E2) in these cochleae; in any cochlear region of implanted control animals (cohort 1); or animals stimulated at 100 µC/cm^2/phase (cohort 2).

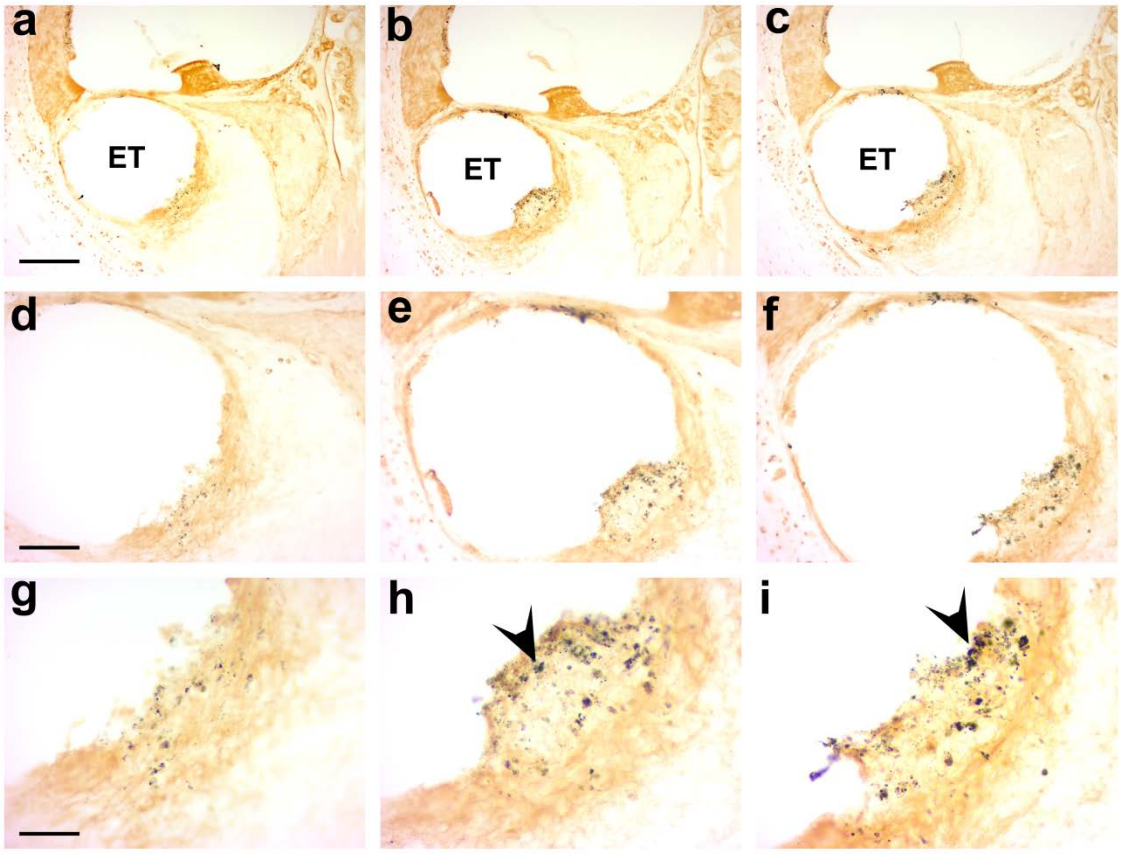

Figure 13. *A series of micrographs taken from the UB turn of a cochlea chronically stimulated at a charge density of 400 μC/cm^2/phase and immunostained with CD 163. Each column is separated by a distance of 36 μm, and descending rows illustrate the electrode tissue capsule at higher magnification. Particulate material localized to the electrode tissue capsule close to the focal necrotic zone is evident (arrowheads). The distribution of this material appears to be quite localized; there is a small amount of deposit in column (a) while much larger deposits are evident in columns (b) & (c), i.e. only 36 or 72 μm distance. ET = electrode tract. Scale bar: a-c, 100 μm; d-f, 50 μm; g-i, 25 μm.*

Histological examination of these particulate deposits revealed they occurred in two forms; the majority of the material appeared to be of sub-micron dimensions and readily phagocytosed by macrophages, while there were occasional larger deposits (~ 20 μm in length) that had not undergone phagocytosis (Fig. 14). This particulate material was identified as Pt using SEM-EDS (Fig. 15).

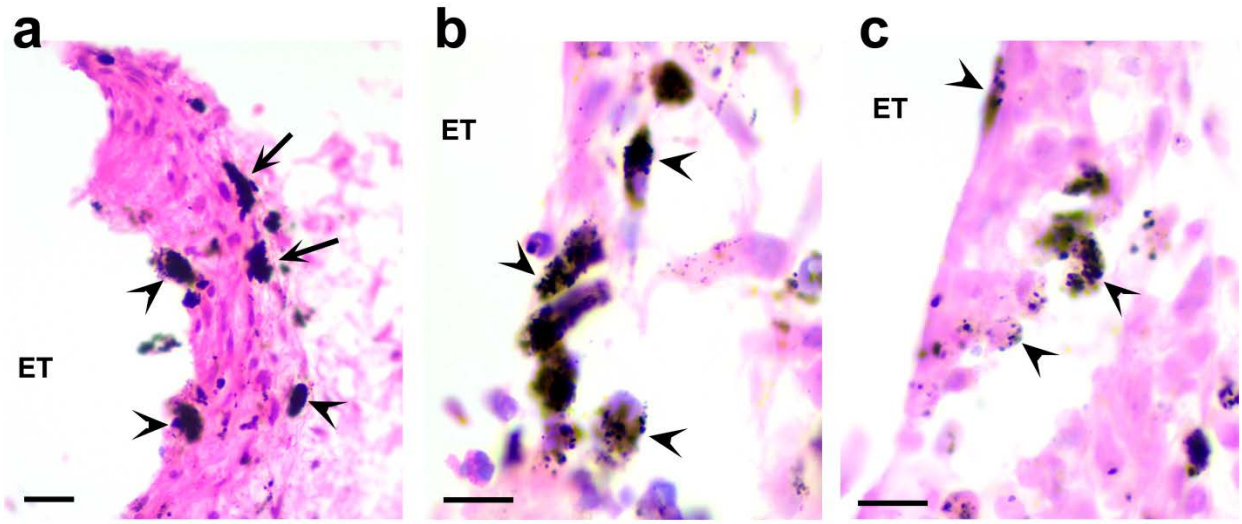

Figure 14. *Representative examples of particulate deposits in the tissue capsule associated with electrodes chronically stimulated at 267 or 400 μC/cm^2/phase. The majority of the deposits are sub-micron in dimensions and readily phagocytosed by macrophages (arrowhead). In many cases the entire macrophage cytoplasm was completely occupied by these sub-micron deposits. Some of the particulate material was much larger and had not undergone phagocytosis (arrows; Fig. 14a). ET = electrode tract. Scale bar: (a) 20 μm; (b) & (c) 10 μm.*

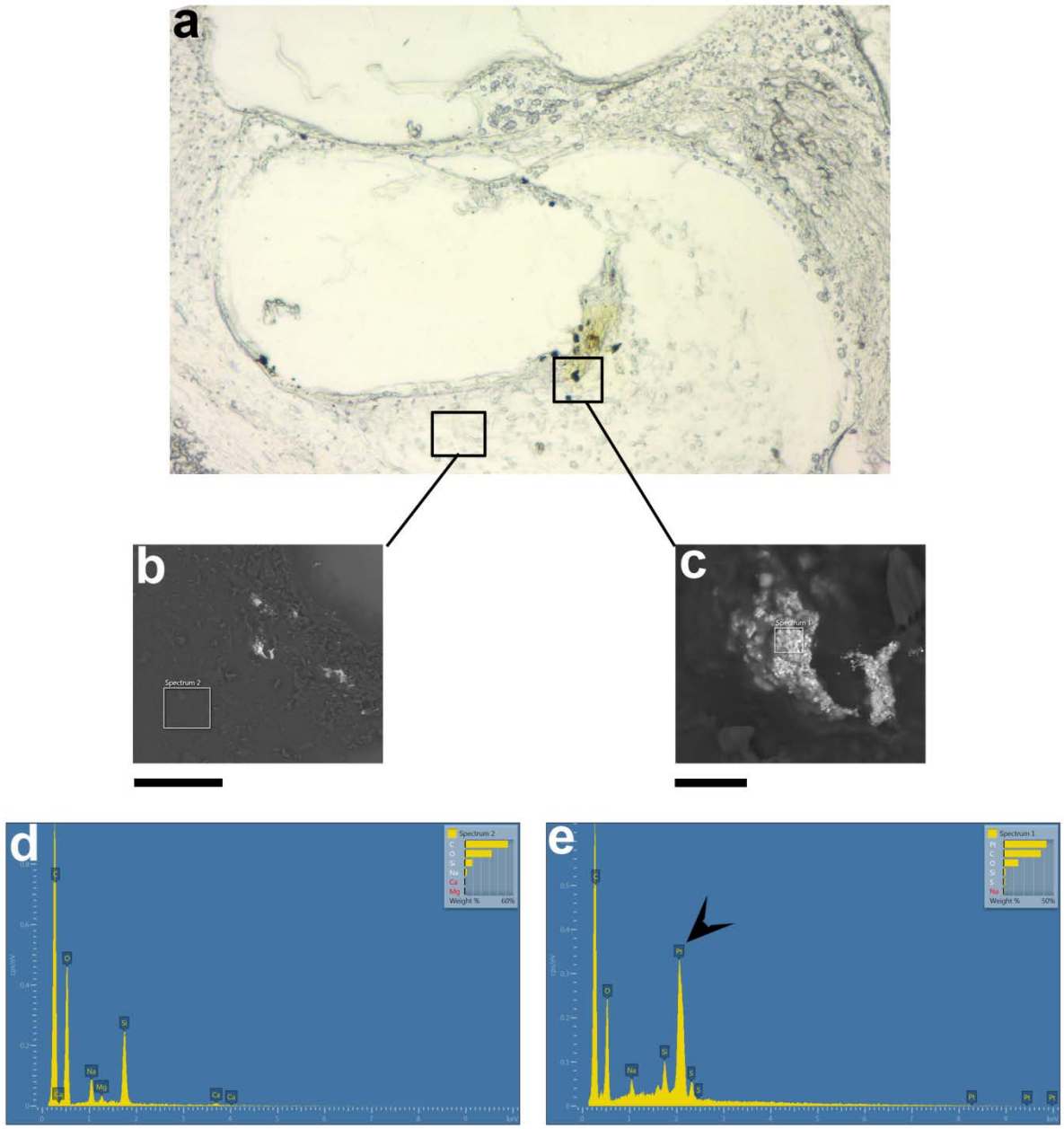

Figure 15. *(a) An unstained section from the UB turn of a cochlea stimulated at 400 μC/cm^2/phase illustrating evidence of particulate material in the electrode tissue capsule. (b & c) Unstained sections imaged in a SEM fitted with an EDS facility. In regions of the tissue capsule devoid of particulate material (b) EDS spectrometry exhibited elemental components typical of organic matter (d). In contrast, regions containing particulate material (c) exhibited clear evidence of Pt in the spectrogram (arrowhead; e) in addition to organic matter. Squares in (a) are not drawn to scale. Scale bar: b = 50 μm; c = 5 μm.*

3.6 Trace analysis of platinum

Trace levels of Pt was identified in cochleae stimulated at the highest stimulus levels used in the present study (400 $\mu C/cm^2$/phase; cohort 4) using ICP-MS (mean = 136 ng per half cochlea). While no evidence of Pt was detected in the contralateral cochleae of this cohort, small but detectible levels of Pt were measured in the chronically implanted unstimulated cochleae (mean = 1.1 ng per half cochlea; cohort 1).

Discussion:

The present study examined the pathophysiological effects of chronic electrical stimulation of smooth Pt electrodes in the guinea pig cochlea at charge densities both within and above currently accepted safe levels (1, 7). Compared with unstimulated control electrodes and electrodes stimulated at 100 $\mu C/cm^2$/phase, stimulation at charge densities of 267 or 400 $\mu C/cm^2$/phase resulted in significant Pt corrosion from the electrode surface. Histological and SEM-EDS examination of cochleae stimulated at these high charge densities indicated the presence of particulate Pt associated with the electrode/tissue interface and was confirmed for the 400 $\mu C/cm^2$/phase cohort using ICP-MS. The extent of a foreign body tissue response within the cochlea was dependent on the degree of electrical stimulation. Control cochleae showed a minimal tissue response, while chronic stimulation at 100 $\mu C/cm^2$/phase evoked a fine tissue capsule surrounded by a mature fibrous tissue response. Cochleae stimulated at 267 or 400 $\mu C/cm^2$/phase exhibited a more extensive tissue response localized to the site of stimulation and included a focal region of necrosis close to the Pt electrode. Despite chronic stimulation at high charge densities inducing significant Pt corrosion, there was no loss of ANs in stimulated cochleae compared with their contralateral controls. Indeed, we report a statistically significant *increase* in AN density proximal to electrodes stimulated at 267 or 400 $\mu C/cm^2$/phase compared to their controls. Finally, there was no evidence of a reduction in AN function associated with chronic stimulation at 100, 267 or 400 $\mu C/cm^2$/phase as evidenced by stable EABR thresholds over the course of the stimulation program.

Tissue response and Pt dissolution

The present study demonstrated that the particulate Pt observed in the cochleae was primarily a product of stimulus induced Pt corrosion rather than flaking of Pt generated during manufacture (17). While we saw no evidence of particulate Pt in the cochleae or evidence of corrosion from the electrodes associated with the implanted unstimulated cochleae (cohort 1), we did observe just-detectable levels of Pt in these cochleae using ICP-MS (1.1 ng per half cochlea). The source of this trace Pt is yet to be determined.

Several recent studies have examined the cochleae of patients following long-term cochlear implant use and have demonstrated evidence of particulate Pt within the electrode tissue capsule (16-19). Clark and colleagues (16, 17) examined the cochlea of one patient who had

used three implants over a thirty year period including a prototype device manufactured at the University of Melbourne, a Cochlear™ Nucleus® N22 Cochlear Implant using bipolar stimulation, and a Cochlear™ Nucleus® CI24 Cochlear Implant that was capable of using either bipolar or monopolar stimulation modes. The Pt corrosion products identified in this cochlea was attributed to possible poor charge recovery associated with the prototype device (17). The cochleae examined by Nadol and colleagues (18, 19) were also long-term implant users (mean years of cochlear implant use: 12.5 and 10.5 years respectively) using a variety of commercial devices. Particulate Pt was observed in all 45 cochlear specimens examined (19) implying that Pt corrosion product is relatively common in cochleae of long-term cochlear implant users and is not associated with a specific implant design.

While the duration of cochlear implant use was far longer in these clinical studies, it is not possible to determine the histopathological effects associated with particulate Pt on ANs and cochlear structures due to the underlying pathology that resulted in the hearing loss. The controlled nature of the present study demonstrated that the release of Pt into the cochlea, at least over a 4 week period, does not result in loss of auditory neurons or adversely affect neural function to electrical stimulation.

In addition to these recent clinical observations, two early reports describe electrode corrosion within a cochlea of a patient that had been implanted for several years with a prototype device that used silver electrodes. Extensive corrosion of the silver electrodes was reported. Dissection of the temporal bone revealed macroscopic evidence of silver corrosion products in the cochlea, while histological analysis revealed a widespread inflammatory response including extensive new bone formation and an almost complete loss of ANs (35, 36). Although it is not possible to accurately establish the relative contribution to the cochlear pathology of the pre-existing disease versus the response to the silver electrodes and their traumatic insertion, it is reasonable to conclude that a significant proportion of the extensive pathology observed was a result of the extensive silver corrosion products.

There are also a number of pre-clinical reports that describe the formation of electrode corrosion products following intracortical stimulation using near-field microelectrodes. Agnew and colleagues directly stimulated the feline cortex for 4.5 days at high charge densities (75-300 $\mu C/cm^2$/phase) using Pt electrodes and reported severe tissue damage "marked by widespread architectural derangement and overall loose appearance of the tissue" (i.e. necrosis) at high charge/phase and charge density (37). Moreover, they reported evidence of "metallic appearance of crystalline deposits" observed in stimulated but not unstimulated tissue that "may be electrolytic deposits of metallic Pt emanating from the Pt electrodes". This work highlights how rapidly both Pt corrosion product and stimulus induced changes to neural tissue, can occur.

Using SEM techniques, studies of chronic intracortical stimulation in experimental animals using either Pt-30%Ir or activated iridium microelectrodes at charge densities over a range of 100-3200 $\mu C/cm^2$/phase showed corrosion of the Pt electrode pulsed for 24 hours or more at charge densities $\geq$ 200 $\mu C/cm^2$/phase (38). Higher charge densities were associated with increased levels of corrosion. Corresponding histological analysis showed evidence of Pt-Ir deposits. Although the maximum stimulus levels (3200 $\mu s/cm^2$/phase; 64 nC/phase) occasionally showed evidence of focal necrosis close to the electrode tip, neural damage was limited. The authors considered this local necrosis was a result of the formation of toxic by-products from the tip of the electrode. The site of necrosis was often associated with metallic deposits containing Pt and Ir, suggesting electrode dissolution was a contributing factor. No damage or tissue necrosis was associated with activated Ir electrodes (38).

We observed regions of focal necrosis in the present study that appeared to be proximal to the stimulating electrodes. This localized tissue response was only observed in animals stimulated at 267 or 400 $\mu C/cm^2$/phase and appeared to have features similar to those described by Agnew and colleagues (38). Although Pt corrosion may have contributed to this focal necrosis, it is likely that other stimulus induced changes in the local electrolyte environment, including changes in pH (11), played a major role.

An interesting finding from this study is that cathodic first electrodes (E4 and E7), which were pulsed to more negative potentials than their resting potential, demonstrated significant levels of corrosion. Pt corrosion has been well studied for anodic reactions such as $Pt + 6Cl^- \Leftrightarrow [PtCl_6]^{2-} + 4e^-$ where thermodynamics favours dissolution under anodic conditions (39, 40). However Pt corrosion, especially under conditions representative of the *in vivo* environment, is known to be complex and not to follow simple thermodynamic principles (41). Recent work has provided some understanding of the anodic dissolution process. It has been shown that as the electrode transitions above and below its oxide formation and reduction regions, place exchange occurs between surface adsorbed oxygen and the Pt lattice. This exchange, particularly in the reduction part of the anodic cycle, disrupts the Pt lattice and appears to release Pt ions into solution during each pulse cycle (42). This mechanism explains the long observed phenomenon that Pt dissolves far more readily under pulsatile conditions than under extremely anodic steady state conditions or monophasic pulsing. The effect of cathodic pulsing on Pt electrodes has received more limited attention (40). Recently, a mechanism of Pt corrosion was demonstrated under mild cathodic pulsing conditions (i.e. -1 V pulses) (43). In this mechanism dissolved oxygen in the electrolyte is reduced during a cathodic pulse by a reaction chain that includes the highly oxidising, short lived, hydroxyl radical ($^{\cdot}OH$). This radical is thought to be responsible for the oxidation of Pt metal to its soluble ionic form (Pt^{2+} or Pt^{4+}). As with anodic pulsing it appears that the transition through a particular voltage window during each pulse is responsible for releasing a defined amount of Pt. The dissolution rate reported for this process under neutral pH conditions is 0.173 ng per pulse per cm^2 (albeit using very different pulse timing

parameters from ours). When, converted to our 4 week experiment with 0.05 mm^2 electrodes, this equates to a Pt loss of around 40 μg. Since we measured an average of 136 ng of soluble Pt for each half cochlea in the 400 $\mu C/cm^2$/phase cohort, this process could easily generate sufficient Pt corrosion product to account for our observations.

The fate of the Pt ions once they leave the metal lattice *in vivo* is not well understood. The observation of particulate Pt in the tissue surrounding electrodes suggests that the Pt has finite but limited mobility. One possible explanation for these particles is that Pt ions are rapidly reduced back onto the bulk Pt electrode during the cathodic pulse. Physical attachment between the reduced Pt and the bulk electrode is not strong, resulting in the electroplated Pt flaking off into the adjacent tissue (Dr Pavel Takmakov; personal communication). There is support from electrochemical studies for Pt redeposition following Pt dissolution and electrode roughening; the amount of Pt redeposited depends on the amount of Pt ions proximal to the electrode when its potential becomes sufficiently negative to reduce Pt ions to Pt (44).

The large (~20 μm long) Pt deposits observed in the present study are consistent with redeposited Pt flaking from the electrode. These deposits had not undergone phagocytosis, presumable due to their size; it remains to be determined whether these large Pt deposits are broken down and phagocytosed. However, the majority of Pt corrosion product observed in the present study were sub-micron in size and readily phagocytosed by macrophages within the tissue capsule. It is unclear at present whether these small Pt deposits are products of the breakdown of Pt flaked from the electrode surface or form via other means.

While we observed no neural loss in the present study, the extent of Pt ions present in the cochlear tissue was unknown. *In vitro* studies of Pt toxicity in cell cultures indicate that Pt ions are significantly more toxic than Pt nanoparticles (22), however our measuring techniques could not differentiate between particulate and ionic Pt. Spiers and colleagues, using synchrotron based X-ray fluorescence microscopy to examine for Pt distribution in a long-term cochlear implant user, reported particulate and nano sized Pt deposits but did not describe evidence of ionic Pt (17).

Finally, while all Pt deposits in the present study appeared to be localized to a stimulating electrode in the scala tympani of the cochlea, it is unclear whether Pt accumulation occurs in other organs. This work is currently under investigation in our laboratory.

Although we did not observe evidence of neural loss in the present study there was a statistically significant increase in the foreign body response associated with electrical stimulation. Tissue growth was evident at 100 $\mu C/cm^2$/phase but more extensive at 267 and 400 $\mu C/cm^2$/phase. While the Pt electrode corrosion product may have contributed to the increased tissue response, we saw no evidence of Pt corrosion at 100 $\mu C/cm^2$/phase, suggesting that electrical stimulation *per se* may be responsible for evoking the increased

tissue response. We have previously described stimulus induced increases in the foreign body response in the absence of Pt dissolution (33), and note that there is evidence from clinical studies that "demonstrated the development of a robust fibrous tissue sheath …closest to the site of electric stimulation" (45).

Relationship to the defined safety limits for Pt electrodes

The Shannon limit has been used for 25 years to help define safe levels of electrical stimulation for neural prostheses (1). While there is no doubt it has been a useful guideline defining the boundary between damaging and non-damaging stimulation, there are limitations on how accurately it can define safety limits outside the limited data set from which it was derived (3-5). We have demonstrated the ability to chronically stimulate cochleae using stimulus parameters outside this limit without causing functional changes or damage to ANs, albeit the results did demonstrate that at stimulus levels close to and above the Shannon limit, Pt dissolution and focal necrosis of the tissue capsule proximal to the electrode was evident. With the caveat that the long-term implications of these stimulus induced changes require further study, the present results demonstrate that the Shannon limit appears to be a conservative measure of the limits of safe stimulation in the cochlea. We are not advocating the abandonment of the Shannon limit; it serves the neural prosthesis community well as a useful guideline. However, its conservative nature under certain circumstances suggests that if stimulus parameters are required that lay outside this limit, bespoke safety studies using appropriately designed chronic studies should be considered for specific applications. Such safety studies are likely to be considered necessary by regulatory agencies.

In addition, cochlear implants voluntarily conform to the AAMI standard for commercial cochlear implants (7). This standard defines the Shannon limit (k=1.75) and also imposes a maximum charge density of 216 $\mu C/cm^2$/phase as the safe stimulation limit for these devices (7). Again, some stimulus parameters used in the present study were at k=1.9 – a value 41% greater in terms of charge or charge density than the AAMI limit and 58% greater than Shannon's proposed "conservative" limit of k=1.5. While these stimulus levels were not damaging to ANs, the fact that some corrosion of Pt from flanker electrodes stimulated at half the charge density of centre electrodes in the tripole occurred (i.e. 200 $\mu C/cm^2$/phase; Fig. 12) indicates that stimulation at the AAMI limit of 216 $\mu C/cm^2$/phase may result in Pt dissolution.

Results from long-term cochlear implant users indicating that Pt corrosion products were evident in all 45 cochleae (19) is of significant interest. While the present study indicates that these products are not damaging to cochlear tissues, the typical charge densities used in a clinical setting would be much lower than the levels used here (median bipolar stimulation: ~ 50 $\mu C/cm^2$/phase; monopolar: ~ 8 $\mu C/cm^2$/phase). Further research is required to investigate the correlation between stimulation intensity, stimulus duration and Pt dissolution *in vivo* (3).

Stimulus induced rescue of ANs

An unexpected outcome of the present study was the statistically significant increase in ANs proximal to the electrode array following chronic stimulation of cochleae at 267 and 400 $\mu C/cm^2$/phase. These results imply the presence of a stimulus induced rescue effect delaying the progression of AN degeneration that normally occurs following hearing loss (34). Although we have not previously observed a stimulus induced rescue effect (23, 46), we have not previously used stimulus levels as high as those used in the present study. Other laboratories have described a stimulus induced rescue effect of ANs, however there did not appear to be a strong relationship between AN rescue and stimulus intensity (47, 48). The mechanism(s) underlying this trophic effect on ANs remains to be determined.

Electrode impedance, electrode surface area and Pt corrosion

We used the peak voltage transient measured at the end of the first phase of a biphasic current pulse to determine electrode impedance. As expected, the impedance increased across cohorts as the electrode surface area was reduced (compare: Fig 3(a), 0.2 mm^2; Fig. 3(b), 0.075 mm^2; and Fig. 3(c), 0.05 mm^2). Interestingly, we saw no evidence of a reduction in impedance for electrodes that had undergone significant Pt dissolution (electrodes 4 & 7; cohorts 3 & 4). While pitting corrosion will produce an increase in surface area, it is possible that any resultant reduction in impedance is nullified by the presence of a more extensive fibrous tissue response proximal to these electrodes. It is also possible that our impedance measurement method may not have been sensitive to the cellular response apparent in the histology. Spectroscopic studies of intracochlear (49), microelectrode (50) and deep brain stimulation (51) electrode impedance changes due to fibrous tissue growth suggest its effects are predominantly observed at frequencies below 1 kHz. In contrast the pulsatile measurement technique used in the present study is most sensitive to frequencies above 1 kHz.

Cochlear implants as an in vivo platform for evaluating novel materials

Cochlear implants provide a useful platform for evaluating the biocompatibility of novel electrode materials and novel electrical stimulation protocols, particularly in the assessment of far-field electrodes (4). Importantly, cochlear implant electrode arrays can be inserted into the fluid-filled scala tympani without trauma to neurons or other tissues (52), and the array is mechanically stable and therefore not subject to repeated movement that can contribute to the inflammatory response associated with electrodes implanted in other sites including the central nervous system (53). Therefore, the foreign body response and associated neural degeneration can be directly related to the biocompatibility of the electrode array and the electrical stimulus.

Novel aspects of the present study

The present study has incorporated a number of important features in order to undertake this research. First, tripolar stimulation was used to ensure that we could stimulate awake, free moving animals chronically at levels tolerated by the animals while achieving the high

charge densities required for this research. Second, we chose to simulate two tripolar sites on the electrode array, thereby providing two electrode sites within the cochlea stimulated at the selected charge density, four flanker electrodes stimulated at half this charge density, and two electrodes that served as unstimulated controls (54). Having two tripolar sites on each electrode array allowed us to examine one site histologically while evaluating the second site for trace analysis of Pt. Finally, the unique electrode fabrication technique used in this study provided accurate Pt electrode contact areas (0.05-0.2 mm^2), allowing for the first time chronic intracochlear electrical stimulation at charge densities as high as 400 $\mu C/cm^2$/phase; above both the electrochemically safe limits for Pt defined from *in vitro* studies (100-300 $\mu C/cm^2$/phase; (39)), the safe charge density limit set by the AAMI as an industry standard for commercial cochlear implants (Shannon k=1.75; 216 $\mu C/cm^2$/phase; (7)).

Clinical implications

Although further studies are required to evaluate the safety of electrical stimulation of Pt electrodes at these high charge densities over several months, the ability to safely stimulate at these levels would expand the range of electrode arrays for clinical application. This would include the use of smaller diameter electrode arrays with reduced electrode contact areas designed to minimize electrode insertion trauma (55), particularly associated with preserving residual hearing (56).

This research also has implications for establishing maximum safe stimulation levels and improved electrode designs for other applications in neurotechnology. For example, electrodes used in deep brain stimulation typically use Pt electrodes with a surface area of ~6 mm^2; smaller electrode contacts that operate within the safety limits for stimulation of central nervous system neurons are expected to reduce the incidence of adverse off-target effects (57). As a second example, retinal prostheses typically require high charge/phase in order to evoke phosphines (58), resulting in the need to use relatively large surface area electrodes or selecting materials with greater charge injection capacity than Pt (e.g. activated iridium).

Acknowledgements:

This work was supported by NIDCD (R01DC015031) and Cochlear Ltd. The Bionics Institute acknowledges support of the Victorian Government through Operational Infrastructure Support Program. We thank Dr A. Thompson, C. Singleton, E. Trang, C. McGowan, B. Flynn, V. Maxim, H. Feng, J. Zhou, N. Critch, C. Gaunt, Dr T. Nguyen, C. Grenness from the Bionics Institute, R. Curtain from the SEM Facility at Bio21, University of Melbourne for their excellent technical assistance, Dr Pavel Takmakov and Prof John Furness for advice on aspects of this study, and staff at the National Measurement Institute of the Australian Government for ICP-MS analysis.

References:

1. Shannon RV. A model of safe levels for electrical stimulation. IEEE Trans Biomed Eng. 1992;39(4):424-6.
2. Merrill DR, Bikson M, Jefferys JG. Electrical stimulation of excitable tissue: design of efficacious and safe protocols. J Neurosci Methods. 2005 Feb 15;141(2):171-98.
3. Cogan SF, Ludwig KA, Welle CG, Takmakov P. Tissue damage thresholds during therapeutic electrical stimulation. J Neural Eng. 2016 Jan 20;13(2):021001.
4. Shepherd RK, Villalobos J, Burns O, Nayagam D. The development of neural stimulators: a review of preclinical safety and efficacy studies. J Neural Eng. 2018 May 14.
5. Kumsa D, Steinke GK, Molnar GF, Hudak EM, Montague FW, Kelley SC, et al. Public Regulatory Databases as a Source of Insight for Neuromodulation Devices Stimulation Parameters. Neuromodulation. [Review]. 2018;21:117-25.
6. Hatsushika S, Shepherd RK, Tong YC, Clark GM, Funasaka S. Dimensions of the scala tympani in the human and cat with reference to cochlear implants. Ann Otol Rhinol Laryngol. 1990 Nov;99(11):871-6.
7. ANSI. Cochlear Implant Systems: Requirements for safety, functional verification, labeling and reliability reporting. ANSI/AAMI CI86:2017. Arlington, VA: AAMI; 2017. p. 169.
8. Brummer SB, McHardy J, Turner MJ. Electrical stimulation with Pt electrodes: Trace analysis for dissolved platinum and other dissolved electrochemical products. Brain Behav Evol. 1977;14(1-2):10-22.
9. McHardy J, Geller D, Brummer SB. An approach to corrosion control during electrical stimulation. Ann Biomed Eng. 1977;5(2):144-9.
10. Black RC, Hannaker P. Dissolution of smooth platinum electrodes in biological fluids. Appl Neurophysiol. 1980;42(6):366-74.
11. Huang CQ, Carter PM, Shepherd RK. Stimulus induced pH changes in cochlear implants: an in vitro and in vivo study. Ann Biomed Eng. 2001;29(9):791-802.
12. Gencoglu A, Minerick A. Chemical and morphological changes on platinum microelectrode surfaces in AC and DC fields with biological buffer solutions. Lab Chip. 2009;9(13):1866-73.
13. Musa S, Rand DR, Bartic C, Eberle W, Nuttin B, Borghs G. Coulometric Detection of Irreversible Electrochemical Reactions Occurring at Pt Microelectrodes Used for Neural Stimulation. Anal Chem. 2011 Jun 1;83(11):4012-22.
14. Robblee LS, McHardy J, Marston JM, Brummer SB. Electrical stimulation with Pt electrodes. V. The effect of protein on Pt dissolution. Biomaterials. 1980;1(3):135-9.
15. Palmer J. In vivo and in vitro testing environments for functional assessment of cochlear implants. Sydney: University of New South Wales; 2017.
16. Clark GM, Clark J, Cardamone T, Clarke M, Nielsen P, Jones R, et al. Biomedical studies on temporal bones of the first multi-channel cochlear implant patient at the university of Melbourne. Cochlear Implants Int. 2014 Jun 10.
17. Spiers K, Cardamone T, Furness JB, Clark JCM, Patrick JF, Clark GM. An X-ray fluorescence microscopic analysis of the tissue surrounding the multi-channel cochlear implant electrode array. Cochlear Implants Int. 2016 2016/05/03;17(3):129-31.
18. Nadol JB, Jr., O'Malley JT, Burgess BJ, Galler D. Cellular immunologic responses to cochlear implantation in the human. Hear Res. 2014 Dec;318:11-7.
19. O'Malley JT, Burgess BJ, Galler D, Nadol JB, Jr. Foreign Body Response to Silicone in Cochlear Implant Electrodes in the Human. Otology & neurotology : official publication of

the American Otological Society, American Neurotology Society [and] European Academy of Otology and Neurotology. 2017 Aug;38(7):970-7.
20. Pascoe JM, Roberts JJ. Interactions between mammalian cell DNA and inorganic platinum compounds. I. DNA interstrand cross-linking and cytotoxic properties of platinum(II) compounds. Biochem Pharmacol. 1974 May 1;23(9):1359-65.
21. McWhinney SR, Goldberg RM, McLeod HL. Platinum neurotoxicity pharmacogenetics. Mol Cancer Ther. 2009 Jan;8(1):10-6.
22. Wissel K, Brandes G, Putz N, Angrisani GL, Thieleke J, Lenarz T, et al. Platinum corrosion products from electrode contacts of human cochlear implants induce cell death in cell culture models. PLoS One. 2018;13(5):e0196649.
23. Shepherd RK, Coco A, Epp SB, Crook JM. Chronic depolarization enhances the trophic effects of brain-derived neurotrophic factor in rescuing auditory neurons following a sensorineural hearing loss. J Comp Neurol. 2005 May 30;486(2):145-58.
24. Landry TG, Fallon JB, Wise AK, Shepherd RK. Chronic neurotrophin delivery promotes ectopic neurite growth from the spiral ganglion of deafened cochleae without compromising the spatial selectivity of cochlear implants. J Comp Neurol. 2013 Aug 15;521(12):2818-32.
25. McCreery DB, Agnew WF, Yuen TG, Bullara L. Charge density and charge per phase as cofactors in neural injury induced by electrical stimulation. IEEE Trans Biomed Eng. 1990;37(10):996-1001.
26. Green RA, Ordonez JS, Schuettler M, Poole-Warren LA, Lovell NH, Suaning GJ. Cytotoxicity of implantable microelectrode arrays produced by laser micromachining. Biomaterials. 2010 Feb;31(5):886-93.
27. Rubinstein JT, Spelman FA, Soma M, Suesserman MF. Current density profiles of surface mounted and recessed electrodes for neural prostheses. IEEE Trans Biomed Eng. 1987;34(11):864-75.
28. Xu J, Shepherd RK, Millard RE, Clark GM. Chronic electrical stimulation of the auditory nerve at high stimulus rates: a physiological and histopathological study. Hear Res. 1997;105:1-29.
29. Senn P. Neurostimulation for the management of pain. [PhD]. Melbourne: University of Melbourne; 2015.
30. George SS, Shivdasani MN, Wise AK, Shepherd RK, Fallon JB. Electrophysiological channel interactions using focused multipolar stimulation for cochlear implants. J Neural Eng. [Research Support, Non-U.S. Gov't]. 2015 Dec;12(6):066005.
31. Patrick JF, Seligman PM, Money DK, Kuzma JA. Engineering. In: Clark GM, Tong YC, Patrick JF, editors. Cochlear Prostheses. Edinburgh: Churchill Livingston; 1990. p. 99-124.
32. Wise AK, Tan J, Wang Y, Caruso F, Shepherd RK. Improved Auditory Nerve Survival with Nanoengineered Supraparticles for Neurotrophin Delivery into the Deafened Cochlea. PLoS One. 2016;11(10):e0164867.
33. Shepherd RK, Wise AK, Enke YL, Carter PM, Fallon JB. Evaluation of focused multipolar stimulation for cochlear implants: a preclinical safety study. J Neural Eng. 2017 Jun 13;14(4):046020.
34. Wise AK, Pujol R, Landry TG, Fallon JB, Shepherd RK. Structural and Ultrastructural Changes to Type I Spiral Ganglion Neurons and Schwann Cells in the Deafened Guinea Pig Cochlea. J Assoc Res Otolaryngol. 2017 Dec;18(6):751-69.
35. Johnsson LG, House WF, Linthicum FH, Jr. Otopathological findings in a patient with bilateral cochlear implants. The Annals of otology, rhinology & laryngology Supplement. 1982 Mar-Apr;91(2 Pt 3):74-89.

36. Johnsson LG, House WF, Linthicum FH. Bilateral cochlear implants: histological findings in a pair of temporal bones. Laryngoscope. 1979;89(5 Pt 1):759-62.
37. Agnew WF, Yuen TG, Pudenz RH, Bullara LA. Electrical stimulation of the brain. IV. Ultrastructural studies. Surg Neurol. 1975;4(5):438-48.
38. Agnew WF, Yuen TG, McCreery DB, Bullara LA. Histopathologic evaluation of prolonged intracortical electrical stimulation. Exp Neurol. 1986;92(1):162-85.
39. Brummer SB, Turner MJ. Electrochemical considerations for safe electrical stimulation of the nervous system with platinum electrodes. IEEE Trans Biomed Eng. 1977;24(1):59-63.
40. Kumsa D, Hudak EM, Montague FW, Kelley SC, Untereker DF, Hahn BP, et al. Electrical neurostimulation with imbalanced waveform mitigates dissolution of platinum electrodes. J Neural Eng. 2016 Sep 21;13(5):054001.
41. Donaldson NN, Donaldson PE. Performance of platinum stimulating electrodes mapped on the limit-voltage plane. Part 2. Corrosion in vitro. Medical & biological engineering & computing. 1986 Jul;24(4):431-8.
42. Topalov AA, Cherevko S, Zeradjanin AR, Meier JC, Katsounaros I, Mayrhofer KJJ. Towards a comprehensive understanding of platinum dissolution in acidic media. Chem Sci. 2014;5(2):631-8.
43. Percival SJ, Dick JE, Bard AJ. Cathodically Dissolved Platinum Resulting from the O-2 and H2O2 Reduction Reactions on Platinum Ultramicroelectrodes. Anal Chem. 2017 Mar 7;89(5):3087-92.
44. Untereker DF, Bruckenstein S. A dissolution-redeposition mechanism for roughening of platinum electrodes by cyclic potential programs. J Electrochem Soc. 1974;121(3):360-2.
45. Ishai R, Herrmann BS, Nadol JB, Jr., Quesnel AM. The pattern and degree of capsular fibrous sheaths surrounding cochlear electrode arrays. Hear Res. 2017 May;348:44-53.
46. Landry TG, Wise AK, Fallon JB, Shepherd RK. Spiral ganglion neuron survival and function in the deafened cochlea following chronic neurotrophic treatment. Hear Res. 2011 Jul 6;282:303-13.
47. Leake PA, Snyder RL, Hradek GT, Rebscher SJ. Consequences of chronic extracochlear electrical stimulation in neonatally deafened cats. Hear Res. 1995;82:65-80.
48. Leake PA, Snyder RL, Hradek GT, Rebscher SJ. Chronic intracochlear electrical stimulation in neonatally deafened cats: effects of intensity and stimulating electrode location. Hear Res. 1992;64:99-117.
49. Duan YY, Clark GM, Cowan RS. A study of intra-cochlear electrodes and tissue interface by electrochemical impedance methods in vivo. Biomaterials. 2004 Aug;25(17):3813-28.
50. Mercanzini A, Colin P, Bensadoun JC, Bertsch A, Renaud P. In vivo electrical impedance spectroscopy of tissue reaction to microelectrode arrays. IEEE transactions on bio-medical engineering. 2009 Jul;56(7):1909-18.
51. Lempka SF, Miocinovic S, Johnson MD, Vitek JL, McIntyre CC. In vivo impedance spectroscopy of deep brain stimulation electrodes. J Neural Eng. 2009 Aug;6(4):046001.
52. Shepherd R, Verhoeven K, Xu J, Risi F, Fallon J, Wise A. An improved cochlear implant electrode array for use in experimental studies. Hear Res. 2011 Jul;277(1-2):20-7.
53. Thelin J, Jorntell H, Psouni E, Garwicz M, Schouenborg J, Danielsen N, et al. Implant size and fixation mode strongly influence tissue reactions in the CNS. PLoS One. 2011;6(1):e16267.

54. Shepherd RK, Carter PM, Enke YL, Wise AK, Fallon JB, editors. Chronic intracochlear electrical stimulation at high charge densities results in Pt dissolution but not neural loss in vivo. Neural Interfaces Conference; 2018 June 25-27; Minneapolis, MN, USA.
55. Helbig S, Helbig M, Leinung M, Stover T, Baumann U, Rader T. Hearing preservation and improved speech perception with a flexible 28-mm electrode. Otology & Neurotology. 2015 Jan;36(1):34-42.
56. Bester CW, Campbell L, Dragovic A, Collins A, O'Leary SJ. Characterizing Electrocochleography in Cochlear Implant Recipients with Residual Low-Frequency Hearing. Frontiers in neuroscience. 2017;11:141.
57. Hickey P, Stacy M. Deep Brain Stimulation: A Paradigm Shifting Approach to Treat Parkinson's Disease. Front Neurosci. 2016;10:173.
58. Shepherd RK, Shivdasani MN, Nayagam DA, Williams CE, Blamey PJ. Visual prostheses for the blind. Trends Biotechnol. 2013 Oct;31(10):562-71.